

Resonance width for a particle-core coupling model with a square-well potential

K. Hagino^{1,2,3}, H. Sagawa^{4,5}, S. Kanaya⁶, and A. Odahara⁶

¹*Department of Physics, Tohoku University, Sendai 980-8578, Japan*

²*Research Center for Electron Photon Science, Tohoku University, 1-2-1 Mikamine, Sendai 982-0826, Japan*

³*Department of Physics, Kyoto University, Kyoto 606-8502, Japan*

⁴*RIKEN Nishina Center, Wako 351-0198, Japan*

⁵*Center for Mathematics and Physics, University of Aizu, Aizu-Wakamatsu, Fukushima 965-8560, Japan*

⁶*Department of Physics, Osaka University, Osaka 560-0043, Japan*

.....
We derive a compact formula for the width of a multi-channel resonance state. To this end, we use a deformed square-well potential and solve the coupled-channels equations. We obtain the S -matrix in the Breit-Wigner form, from which partial widths can be extracted. We apply the resultant formula to a deformed nucleus and discuss the behavior of partial width for an s -wave channel.
.....

Subject Index D13,D29

1. Introduction

Much attention has been paid recently to the study of unbound states in nuclei near the neutron and proton drip lines, stimulated by the rapid progress of radioactive ion beam experiments [1–3]. This applies both to unbound nuclei beyond the drip lines and to states in bound nuclei above the threshold of a particle emission. A particular interest is in single-particle resonance states, which decay to a neighboring nucleus by emitting one nucleon. Such resonances also have a large impact on the r -process and rp -process nucleosyntheses. Bohr and Mottelson have derived a simple formula for the width of a single-particle resonance state using a spherical square-well potential [4]. The formula has been used, e.g., in Ref. [5].

In this paper, we extend the formula derived by Bohr and Mottelson to multi-channel resonances. That is, we discuss resonances in a particle-core system, in which several angular momentum components are coupled together due to excitations of the core nucleus. Such channel coupling effects have been known to play an important role in one nucleon decays of unbound nuclei [6–14] (see also Ref. [15] for a two-proton decay). Single-particle resonances in a deformed potential have also been discussed, e.g., in Refs. [16–19]. In particular, the coupling between s -wave and d -wave components often plays a crucial role in neutron-rich nuclei close to the drip-line [18, 19]. The extended formula presented in this paper will provide a simple estimate of partial and total widths for such multi-channel resonance states.

The paper is organized as follows. In Sec. II, we consider a spherical square-well potential and summarize the formula of Bohr and Mottelson. In Sec. III, we extend the formula to multi-channel cases. We apply the extended formula to a deformed nucleus by taking into

account the rotational excitations of the core nucleus, which results in a mixture of s and d waves. We discuss the partial width of the s -wave channel, for which a resonance may not exist in the absence of the coupling to the d -wave component. We then summarize the paper in Sec. IV.

2. Spherical square-well potential

In this paper, we consider a two-body system with a neutron and a core nucleus. Let us first consider a positive energy state of the system in a spherical square-well potential given by,

$$V(r) = V_0 \theta(R - r), \quad (1)$$

where $V_0 (< 0)$ and R are the depth and the range of the potential, respectively. Here, $\theta(x)$ is the step function.

We shall closely follow Ref. [4] and derive the S -matrix for this potential. Writing the wave function for the relative motion as

$$\Psi(\mathbf{r}) = \frac{u_l(r)}{r} Y_{lm}(\hat{\mathbf{r}}), \quad (2)$$

where l and m are the orbital angular momentum and its z component, respectively, and $Y_{lm}(\hat{\mathbf{r}})$ is the spherical harmonics, the Schrödinger equation for the radial wave function, $u_l(r)$, reads,

$$\left(-\frac{\hbar^2}{2\mu} \frac{d^2}{dr^2} + V(r) + \frac{l(l+1)\hbar^2}{2\mu r^2} - E \right) u_l(r) = 0, \quad (3)$$

where μ is the reduced mass and $E (> 0)$ is the energy. The solution of this equation with the spherical square-well potential reads

$$u_l(r) = A_l K r j_l(Kr) \quad (r < R), \quad (4)$$

$$= kr h_l^{(-)}(kr) - U_l(E) kr h_l^{(+)}(kr) \quad (r \geq R), \quad (5)$$

with $K = \sqrt{\frac{2\mu}{\hbar^2}(E - V_0)}$ and $k = \sqrt{\frac{2\mu}{\hbar^2}E}$. Here, A_l is a constant and U_l is the S -matrix, which are given in terms of the phase shift δ_l as $U_l = e^{2i\delta_l}$. $h_l^{(\pm)}(x)$ is the spherical Hankel functions, which are given by $h_l^{(\pm)}(x) = -n_l(x) \pm i j_l(x)$ using the spherical Bessel function, $j_l(x)$, and the spherical Neumann function, $n_l(x)$ [20].

From Eq. (5), one obtains

$$U_l = \frac{L_l - S_l + iP_l}{L_l - S_l - iP_l} e^{2i\phi_l}, \quad (6)$$

where

$$L_l \equiv R \left(\frac{d}{dr} u_l(r) \right)_{r=R} \frac{1}{u_l(R)}, \quad (7)$$

is the logarithmic derivative of the wave function at $r = R$. Notice that the logarithmic derivative of the wave function is continuous at $r = R$, and L_l can be evaluated using either

Eq. (4) or Eq. (5). S_l and P_l in Eq. (6) are defined as,

$$S_l = \frac{G_l(R)G'_l(R) + F_l(R)F'_l(R)}{G_l(R)^2 + F_l(R)^2}, \quad (8)$$

$$P_l = \frac{G_l(R)F'_l(R) - F_l(R)G'_l(R)}{G_l(R)^2 + F_l(R)^2} = \frac{kR}{G_l(R)^2 + F_l(R)^2}, \quad (9)$$

respectively. Here, we have followed Ref. [4] and introduced shorthanded notations defined as,

$$F_l(r) \equiv kr j_l(kr), \quad G_l(r) \equiv -kr n_l(kr), \quad (10)$$

$$F'_l(r) \equiv R \frac{dF_l}{dr}, \quad G'_l(r) \equiv R \frac{dG_l}{dr}. \quad (11)$$

Note that S_l in Eq. (8) and P_l in Eq. (9) correspond to the shift function and the penetrability in the R-matrix method, respectively [22–25]. The phase factor $e^{2i\phi_l}$ in Eq. (6) is the hard sphere scattering term (which is a part of the background S -matrix) given by

$$e^{2i\phi_l} = \frac{G_l(R) - iF_l(R)}{G_l(R) + iF_l(R)}. \quad (12)$$

Notice that the same formulas can be applied to a proton case by replacing the spherical Bessel and Neumann functions in Eqs. (10) and (11) with the corresponding Coulomb wave functions. In this case, the potential $V(r)$ is given by,

$$V(r) = V_0\theta(R - r) + \frac{Ze^2}{r}\theta(r - R), \quad (13)$$

where Z is the charge number of the core nucleus.

A resonance energy, E_r , may be approximately defined as the energy at which $L_l - S_l$ in the denominator in Eq. (6) vanishes, that is, $L_l(E_r) - S_l(E_r) = 0$. Expanding the quantity $L_l - S_l$ around this energy as,

$$L_l(E) - S_l(E) \sim L_l(E_r) - S_l(E_r) - \frac{1}{\gamma_l^2}(E - E_r) = -\frac{1}{\gamma_l^2}(E - E_r), \quad (14)$$

with

$$-\frac{1}{\gamma_l^2} \equiv \left[\frac{d}{dE}(L_l - S_l) \right]_{E=E_r}, \quad (15)$$

one obtains

$$U_l = e^{2i\delta_l} = \left(1 - \frac{i\Gamma_l}{E - E_r + i\frac{\Gamma_l}{2}} \right) e^{2i\phi_l}, \quad (16)$$

where the resonance width Γ_l is defined as

$$\Gamma_l \equiv 2P_l\gamma_l^2. \quad (17)$$

If one neglects the background phase shift, ϕ_l , the S -matrix is $U_l = -1$ at $E = E_r$, which is equivalent to $\delta_l = \pi/2$. Notice that, because of the presence of the background phase shift, in general the resonance energy, E_r , deviates from the energy at which the phase shift, δ_l , passes through $\pi/2$. This is the case especially for a broad resonance, for which the deviation is significant and thus the phase shift does not cross $\pi/2$ at the resonance. That is, $\delta_l = \pi/2$ is not equivalent to the resonance condition, unless the energy dependence of the background

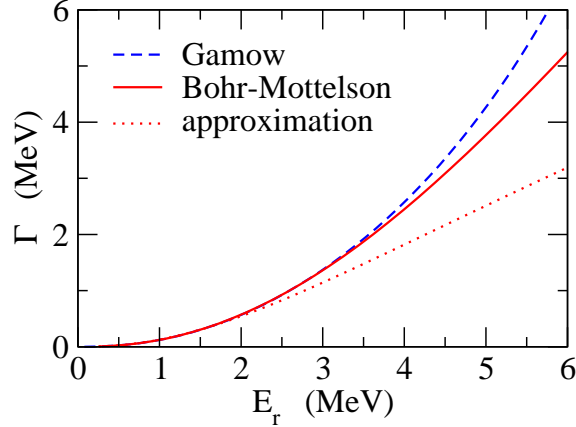


Fig. 1 The resonance widths for d -wave scattering in the mass region of $A \sim 30$ as a function of the resonance energy. Here, the depth of the square-well potential, V_0 , is varied to obtain different resonance energies, E_r . The solid line is obtained with the present method, while the dashed line is obtained by seeking the Gamow state with a complex energy. The dotted lines denote the results of the approximate formula, Eq. (22), for the resonance width for a square-well potential.

phase shift is negligible within the resonance width. In that case, one may alternatively locate the resonance energy as the energy at which the energy derivative of the phase shift takes a maximum as a function of energy [17], since the background phase shift is expected to be a slow function of energy.

A care must be taken for an s -wave scattering. In this case, one would not expect to have a resonance since there is no centrifugal barrier. For a shallow square-well potential, the condition $L_0(E_r) - S_0(E_r) = 0$ may be satisfied at some energy E_r . Even in that situation, however, the background phase shift is large and the total phase shift, δ_0 , would not show a clear resonance behavior. Especially, the phase shift would not pass through $\pi/2$. For a deeper potential, the phase shift may pass through $\pi/2$, but, for s -wave scattering, it is always downwards in energy [26]. It is then misleading to call it a physical resonance state.

Notice that in the present method a pole of the S -matrix is approximately obtained by neglecting the term $-iP_l$ in the denominator in Eq. (6) to determine the resonance energy, E_r . This procedure is justified when the resonance width is small. Figure 1 shows a comparison between the resonance widths for d -wave scattering obtained with two different methods. To this end, we take the radius parameter in the square-well potential as $R = 3.95$ fm and vary the depth parameter, V_0 , from -27 MeV to -21 MeV. The mass μ is taken to be $\mu = 30m_N/31$, where m_N is the neutron mass, in order to simulate a nucleus in the mass region of $A \sim 30$. The dashed line in the figure is obtained by seeking the resonance pole without an approximation. To this end, we impose the outgoing boundary condition to the radial wave function with a complex energy, $E = E_r - i\Gamma/2$. The solid line, on the other hand, is obtained with the present method by seeking the resonance energy which satisfies $L_l(E_r) - S_l(E_r) = 0$. The resonance width is then evaluated according to Eqs. (15) and (17). To this end, the logarithmic derivative, L_l , is evaluated using the wave function for $r < R$

as,

$$L_l = 1 + KR \frac{j'_l(KR)}{j_l(KR)}, \quad (18)$$

from which the energy derivative of L_l is computed as [4]

$$\left. \frac{\partial L_l}{\partial E} \right|_{E=E_r} = -\frac{\mu R^2}{\hbar^2} \left[1 - \frac{l(l+1)}{K^2 R^2} + \frac{S_l(S_l-1)}{K^2 R^2} \right]. \quad (19)$$

The energy derivative of S_l in Eq. (15) is simply computed in a numerical manner.

In Fig. 1, one can see that the resonance width obtained with the present method behaves qualitatively the same as that obtained with the complex energy method, although the former width tends to be smaller than the latter width. See also Appendix A for a comparison of the resonance widths obtained with the square-well potential to those with a smooth Woods-Saxon potential.

An approximate formula for the resonance width, Eq. (17), has been derived in Ref. [4] using the approximate forms of the spherical Bessel and Neumann functions [21],

$$j_l(x) \sim \frac{x^l}{(2l+1)!!} \left(1 - \frac{\frac{1}{2}x^2}{2l+3} + \dots \right), \quad (20)$$

$$n_l(x) \sim -\frac{(2l-1)!!}{x^{l+1}} \left(1 - \frac{\frac{1}{2}x^2}{1-2l} + \dots \right), \quad (21)$$

which are valid for $x \ll 1$. The resultant formula reads [4],

$$\gamma_l^2 \sim \frac{\hbar^2}{\mu R^2} \frac{2l-1}{2l+1} \quad (l \neq 0, \quad kR \ll 1). \quad (22)$$

This formula has the same dependence on the radius R and the reduced mass μ as the so called Wigner limit for the resonance width [22]. However, the underlying model wave function is completely different. That is, the Wigner limit is obtained with a constant wave function, which would be valid for a non-resonant state, while Eq. (22) is obtained with a wave function at a resonance condition, which has a large spatial variation. Notice that Eq. (22) is not applicable for $l = 0$. Even though a different form of the approximate formula can be derive for $l = 0$ [4], we do not discuss it here since an s -wave hardly forms a resonance in the single-channel problem.

The resonance widths evaluated with the simple approximate formula, Eq. (22), are shown by the dotted line in Fig. 1. One can see that the approximate formula indeed works well for small values of the resonance energy, i.e., for narrow resonances, while the deviation from the exact calculation (the solid line) becomes significantly large for broad resonances.

We notice that the results of the square-well potential are not sensitive to the value of the depth parameter, V_0 . In order to demonstrate this, Fig. 2 shows the results obtained with a fixed value of V_0 , that is, $V_0 = -27$ MeV (the filled circles). Notice that Eq. (19) and dS_l/dE are functions of energy $E = E_r$ for a given value of V_0 . We simply vary the energy, E_r , in order to evaluate the resonance width, even though the resonance condition, $L_l(E_r) - S_l(E_r) = 0$, may not be satisfied. The solid and the dotted lines are the same as those in Fig. 1. One can see that the filled circles closely follow the solid line in the region shown in the figure. The approximate formula, Eq. (22), is independent of the depth parameter. The figure indicates that the resonance width is not sensitive to the value of V_0 even outside the region in which

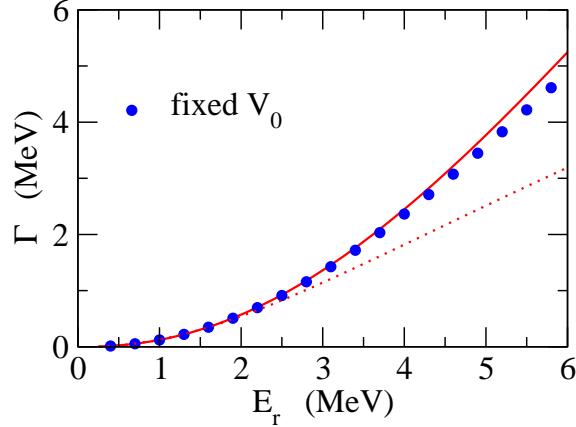


Fig. 2 The resonance width obtained by fixing the value of the depth parameter of the square-well potential (the filled circles) for the same setting as in Fig. 1. The meanings of the solid and the dotted lines are the same as in Fig. 1.

the approximate formula works (that is, $E_r \gtrsim 2$ MeV). This is an advantage to use the spherical square-well potential, as one does not have to consider the consistency between the potential depth and the resonance energy. That is, the resonance width can be evaluated easily for a given resonance energy as an input by taking an arbitrary (but still a reasonable) value for the depth parameter. Unfortunately, this advantage disappears in multi-channel cases, as we discuss in the next section.

3. Resonance in a particle-core coupling model

Let us now extend the formula for the resonance width discussed in the previous section to a multi-channel case. To this end, we consider a system with a particle coupled to the quadrupole motion of a core nucleus, whose potential is given by [18, 26],

$$V(\mathbf{r}) = V_0 \theta \left(R + R \sum_m \alpha_{2m} Y_{2m}^*(\hat{\mathbf{r}}) - r \right), \quad (23)$$

$$\sim V_0 \theta(R - r) + V_0 R \sum_m \alpha_{2m} Y_{2m}^*(\hat{\mathbf{r}}) \delta(R - r), \quad (24)$$

where α_{2m} is the collective coordinate for the quadrupole motion of the core nucleus. Notice that for simplicity we have expanded the potential up to the first order of α_{2m} .

We expand the total wave function as

$$\Psi_{\alpha_0}(\mathbf{r}) = \sum_{\alpha} \frac{u_{\alpha\alpha_0}(r)}{r} |\alpha\rangle, \quad (25)$$

where α_0 denotes the entrance channel (see Eq. (33) below) and the channel wave function $|\alpha\rangle$ is given by

$$|\alpha\rangle \equiv |(ljI_c)IM\rangle = \sum_{m_j, M_c} \langle jm_j I_c M_c | IM \rangle |\phi_{I_c M_c}\rangle |\mathcal{Y}_{jlm_j}\rangle. \quad (26)$$

Here, $\mathbf{j} = \mathbf{l} + \mathbf{s}$ is the total single-particle angular momentum, I_c and M_c are the angular momentum and its z -component of the core nucleus, respectively. I and M are the total angular momentum of the system and its z -component, respectively, which are both conserved.

In Eq. (26), $|\phi_{I_c M_c}\rangle$ and $\mathcal{Y}_{j l m_j}(\hat{\mathbf{r}})$ are the wave function for the core nucleus and the spin-angular wave function for the valence particle, respectively. When there is no spin-dependent interaction, such as the spin-orbit interaction, the spin quantum number is conserved, and one can alternatively use the channel wave function given by

$$|\alpha\rangle \equiv |(I_c)IM\rangle = \sum_{m_l, M_c} \langle l m_l I_c M_c | IM \rangle |\phi_{I_c M_c}\rangle |Y_{l m_l}\rangle. \quad (27)$$

We shall use throughout the paper the general notation $|\alpha\rangle$ for the channel wave functions, which denote either Eq. (26) or (27). The coupled-channels equations for the wave functions $u_{\alpha\alpha_0}(r)$ then read,

$$\left[-\frac{\hbar^2}{2\mu} \frac{d^2}{dr^2} + V_0 \theta(R-r) + \frac{l_\alpha(l_\alpha+1)\hbar^2}{2\mu r^2} + \epsilon_\alpha - E \right] u_{\alpha\alpha_0}(r) \\ = -V_0 R \delta(r-R) \sum_{\alpha'} \langle \alpha | \sum_m \alpha_{2m} Y_{2m}^*(\hat{\mathbf{r}}) | \alpha' \rangle u_{\alpha'\alpha_0}(r) \quad (28)$$

$$\equiv -\delta(r-R) \sum_{\alpha'} C_{\alpha\alpha'} u_{\alpha'\alpha_0}(r), \quad (29)$$

with

$$C_{\alpha\alpha'} \equiv V_0 R \langle \alpha | \sum_m \alpha_{2m} Y_{2m}^*(\hat{\mathbf{r}}) | \alpha' \rangle. \quad (30)$$

Here, ϵ_α is the excitation energy of the core state, $|\phi_{I_c M_c}\rangle$. The explicit form of the coupling term, Eq. (30), is given in Appendices B and C both for rotational and vibrational cases. The solution of the coupled-channels equations for $r < R$ is given as,

$$u_{\alpha\alpha_0}(r) = A_{\alpha\alpha_0} K_\alpha r j_{l_\alpha}(K_\alpha r) \quad (r < R), \quad (31)$$

with $K_\alpha = \sqrt{\frac{2\mu}{\hbar^2}(E - V_0 - \epsilon_\alpha)}$. Using the diagonal matrix $\tilde{\mathbf{F}}(r)$ defined as

$$\tilde{F}_{\alpha\alpha'}(r) = K_\alpha r j_{l_\alpha}(K_\alpha r) \delta_{\alpha,\alpha'}, \quad (32)$$

Eq. (31) is also written in a matrix form as $\mathbf{u}(r) = \tilde{\mathbf{F}}(r)\mathbf{A}$, where $\mathbf{u}(r)$ and \mathbf{A} are the matrices whose components are given by $u_{\alpha\alpha'}(r)$ and $A_{\alpha\alpha'}$, respectively. The solution of the coupled-channels equations for $r \geq R$, on the other hand, is given by,

$$u_{\alpha\alpha_0}(r) = k_\alpha r h_{l_\alpha}^{(-)}(k_\alpha r) \delta_{\alpha,\alpha_0} - \sqrt{\frac{k_{\alpha_0}}{k_\alpha}} U_{\alpha\alpha_0} k_\alpha r h_{l_\alpha}^{(+)}(k_\alpha r) \quad (r \geq R), \quad (33)$$

where $U_{\alpha\alpha_0}$ is the S -matrix and k_α is defined as $k_\alpha = \sqrt{2\mu(E - \epsilon_\alpha)/\hbar^2}$. The matching conditions of the wave functions at $r = R$ are given by,

$$\mathbf{u}(R_<) = \mathbf{u}(R_>), \quad (34)$$

$$-\frac{\hbar^2}{2\mu}(\mathbf{u}'(R_>) - \mathbf{u}'(R_<)) = -\mathbf{C}\mathbf{u}(R), \quad (35)$$

where the prime denotes the radial derivative and $R_>$ and $R_<$ are defined as $R + \epsilon$ and $R - \epsilon$, respectively, with ϵ being an infinitesimally small number. Notice that because of the delta function in Eq. (29) the derivative of the wave functions is not continuous at $r = R$.

When the core nucleus is excited to the channel α , the relative energy decreases by ϵ_α . Such excitation is kinematically allowed only for $E > \epsilon_\alpha$. Those channels which satisfy this

condition are referred to as open channels. For the channels with $E < \epsilon_\alpha$, the excitations are kinematically forbidden and those channels are called closed channels. Even in this case, the *virtual* excitations are still possible, which can influence the dynamics of the open channels. For a closed channel, the channel wave number, k_α , becomes imaginary, $i\kappa_\alpha$, and the first term on the right hand side of Eq. (33) diverges asymptotically. This wave function is thus unphysical. Nevertheless, the same form of wave functions can be formally employed, if the physical S -matrix is restricted to the $n \times n$ submatrix of S , where n is the number of open channels [28].

As in the spherical case, the wave functions for $r \geq R$, Eq. (33), can be solved for the matrix \tilde{U} , whose components are defined as $\tilde{U}_{\alpha\alpha'} = \sqrt{k_{\alpha'}/k_\alpha} U_{\alpha\alpha'}$, and one obtains (see Eq. (6)),

$$\tilde{U} = (\mathbf{G}(R) + i\mathbf{F}(R))^{-1}(\mathbf{L}_> - \mathbf{S} - i\mathbf{P})^{-1}(\mathbf{L}_> - \mathbf{S} + i\mathbf{P})(\mathbf{G}(R) - i\mathbf{F}(R)), \quad (36)$$

where $\mathbf{G}(r)$, $\mathbf{F}(r)$, \mathbf{S} , \mathbf{P} are diagonal matrices whose diagonal components are given by $G_{l_\alpha}(r)$, $F_{l_\alpha}(r)$, S_{l_α} , and P_{l_α} , respectively (see Eqs. (8), (9), and (10)). $\mathbf{L}_>$ is the logarithmic derivative of the wave functions [27],

$$\mathbf{L} \equiv R \left(\frac{d}{dr} \mathbf{u}(r) \right)_{r=R} \mathbf{u}^{-1}(r), \quad (37)$$

evaluated with the wave functions for $r \geq R$. Because of the matching conditions, Eqs. (34) and (35), $\mathbf{L}_>$ is related to $\mathbf{L}_<$ (that is, the logarithmic derivative evaluated with the wave functions for $r < R$) as,

$$\mathbf{L}_> = \frac{2\mu R}{\hbar^2} \mathbf{C} + \mathbf{L}_<. \quad (38)$$

Notice that $\mathbf{L}_<$ is a diagonal matrix, whose components are given by

$$(L_<)_{\alpha\alpha'} = \frac{\tilde{F}'_{l_\alpha}(R)}{\tilde{F}_{l_\alpha}(R)} \delta_{\alpha,\alpha'}, \quad (39)$$

with $\tilde{F}'_l(r) \equiv R d(\tilde{F}_l(r))/dr$.

Noticing that $\mathbf{L}_> - \mathbf{S} + i\mathbf{P} = \mathbf{L}_> - \mathbf{S} - i\mathbf{P} + 2i\mathbf{P}$ and the fact that the matrix $(\mathbf{G}(R) + i\mathbf{F}(R))^{-1}(\mathbf{G}(R) - i\mathbf{F}(R))$ is diagonal with the diagonal elements given by Eq. (12), Eq. (36) can be transformed to

$$\begin{aligned} \tilde{U}_{\alpha\alpha'} &= e^{2i\phi_{l_\alpha}} \delta_{\alpha,\alpha'} \\ &+ 2i(G_{l_\alpha}(R) + iF_{l_\alpha}(R))^{-1}(\mathbf{L}_> - \mathbf{S} - i\mathbf{P})_{\alpha\alpha'}^{-1} P_{\alpha'} (G_{l_\alpha}(R) - iF_{l_\alpha}(R)). \end{aligned} \quad (40)$$

If we write $G_l(R) - iF_l(R) = \sqrt{G_l(R)^2 + F_l(R)^2} e^{i\phi_l}$ and use Eq. (9), the matrix elements of S then read,

$$U_{\alpha\alpha'} = e^{2i\phi_{l_\alpha}} \delta_{\alpha,\alpha'} + 2ie^{i\phi_{l_\alpha}} \sqrt{P_\alpha} (\mathbf{L}_> - \mathbf{S} - i\mathbf{P})_{\alpha\alpha'}^{-1} \sqrt{P_{\alpha'}} e^{i\phi_{l_{\alpha'}}}. \quad (41)$$

We next rewrite the matrix $(\mathbf{L}_> - \mathbf{S} - i\mathbf{P})^{-1}$ as

$$(\mathbf{L}_> - \mathbf{S} - i\mathbf{P})^{-1} = (1 - i(\mathbf{L}_> - \mathbf{S})^{-1}\mathbf{P})^{-1}(\mathbf{L}_> - \mathbf{S})^{-1}. \quad (42)$$

Note that the inverse of the matrix $\mathbf{L}_> - \mathbf{S}$ can be written as,

$$(\mathbf{L}_> - \mathbf{S})^{-1} = \frac{\text{cof}(\mathbf{L}_> - \mathbf{S})}{\det(\mathbf{L}_> - \mathbf{S})}, \quad (43)$$

where $\det(\mathbf{A})$ denotes the determinant of the matrix \mathbf{A} while $\text{cof}(\mathbf{A})$ is the cofactor matrix transposed, that is,

$$\det(\mathbf{A}) = \sum_j A_{ij} \text{cof}(\mathbf{A})_{ji}, \quad (44)$$

for any i . Suppose that the determinant $\det(\mathbf{L}_{>} - \mathbf{S})$ is zero at $E = E_r$. Then, around this energy the inverse of $\mathbf{L}_{>} - \mathbf{S}$ is approximately given by,

$$(\mathbf{L}_{>} - \mathbf{S})^{-1} \sim -\frac{\text{cof}(\mathbf{L}_{>} - \mathbf{S})|_{E=E_r}}{d} \frac{1}{E - E_r}, \quad (45)$$

where the coefficient d is defined as (see Eq. (15)),

$$d \equiv -\frac{d}{dE} \det(\mathbf{L}_{>} - \mathbf{S})|_{E=E_r}. \quad (46)$$

Notice that Eq. (44) indicates that when $\det(\mathbf{A}) = 0$ the elements of a matrix $\text{cof}(\mathbf{A})$ is given in a separable form as $\text{cof}(\mathbf{A})_{ij} = c_i y_j$, where c_i is a constant and the vector \mathbf{y} satisfies $\mathbf{A}\mathbf{y} = 0$. The matrix $\mathbf{L}_{>} - \mathbf{S}$ is a real symmetric matrix and one can choose the normalization of the vector \mathbf{y} such that [28]

$$(\mathbf{L}_{>} - \mathbf{S})_{\alpha\alpha'}^{-1} \sim -\frac{\gamma_\alpha \gamma_{\alpha'}}{E - E_r}, \quad (47)$$

with

$$\gamma_\alpha^2 = -\frac{[\text{cof}(\mathbf{L}_{>} - \mathbf{S})|_{E=E_r}]_{\alpha\alpha}}{\frac{d}{dE} \det(\mathbf{L}_{>} - \mathbf{S})|_{E=E_r}}. \quad (48)$$

Using Eqs. (41), (42), and (47), one finally obtains

$$U_{\alpha\alpha'} = e^{i\phi_{l_\alpha}} \left(\delta_{\alpha,\alpha'} - i \frac{\sqrt{\Gamma_\alpha} \sqrt{\Gamma_{\alpha'}}}{E - E_r + i \frac{\Gamma_{\text{tot}}}{2}} \right) e^{i\phi_{l_{\alpha'}}}, \quad (49)$$

with

$$\Gamma_\alpha = 2\gamma_\alpha^2 P_\alpha, \quad (50)$$

and

$$\Gamma_{\text{tot}} = \sum_\alpha \Gamma_\alpha. \quad (51)$$

This is a well known Breit-Wigner formula for a multi-channel resonance (see, e.g., Refs. [22–24, 29, 30]). One may also regard this as a special case of the R -matrix formula.

Notice that a resonance width for a deformed potential, $V(\mathbf{r}) = V_0 \theta(R + R\beta_2 Y_{20}(\hat{\mathbf{r}}) - r)$ [18], can be also evaluated with exactly the same formula using the channel wave functions of $|\alpha\rangle = |Y_{lK}\rangle$, K being the z -component of the angular momentum, and setting all ϵ_α to be zero in Eq. (28). In this case, the matrix elements of the coupling potential, Eq. (30), are given as $C_{\alpha\alpha'} = V_0 R \langle Y_{lK} | Y_{20} | Y_{l'K} \rangle$ [18].

The upper panel of Fig. 3 shows the result of a two-channel calculation. For this purpose, we consider the rotational coupling with the basis given by Eq. (27) with the total angular momentum of $I = 0$ (see Appendices B and C), that is, a two channel coupling between $|0^+ \otimes s\rangle$ and $||2^+ \otimes d\rangle^{(I=0)}$. The core nucleus is assumed to be ^{30}Mg , and we take ϵ_2 to be the excitation energy of the first 2^+ state, that is, 1.48 MeV. The deformation parameter β_2 is estimated to be $\beta_2 = 0.21$ by using Eq. (B10) in Appendix B with the measured $B(E2)$ value, $B(E2) \uparrow = 241(31)e^2\text{fm}^4$ [34] (see also Ref. [35]) and the radius of $R = 5.1$ fm (that is,

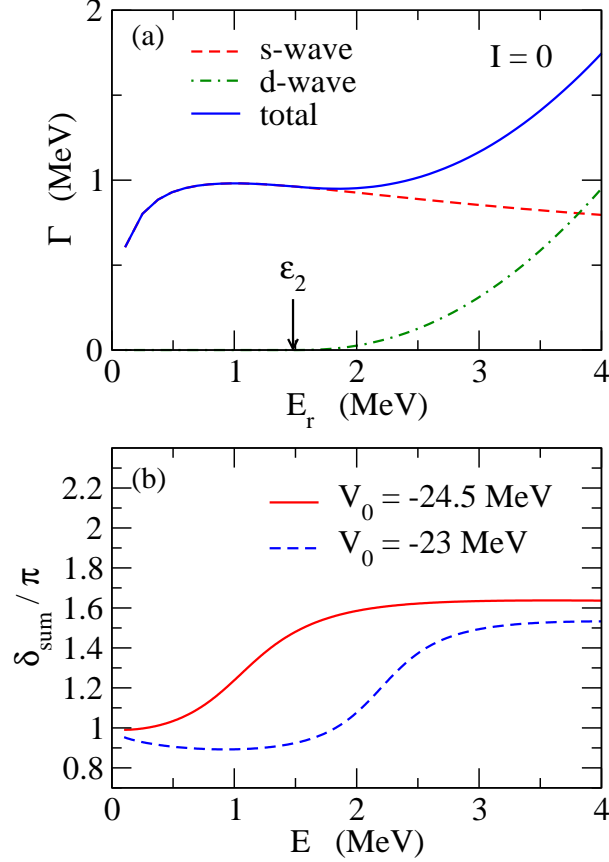


Fig. 3 (The upper panel) The resonance widths for a two-channel rotational coupling with the total angular momentum $I = 0$ as a function of the resonance energy, E_r . Here, the depth of the square-well potential, V_0 , is varied to obtain different resonance energies, E_r . The dashed and the dot-dashed lines show the partial widths for the $|0^+ \otimes s\rangle$ and $[[2^+ \otimes d]^{(I=0)}\rangle$ channels, respectively. The threshold energy for the d -wave channel ($\epsilon_2 = 1.48$ MeV) is also denoted by the arrow. The solid line shows the total width. (The lower panel) The eigenphase sums as a function of energy, E . The solid line is obtained with $V_0 = -24.5$ MeV for the depth of the square well potential, while the dashed line is obtained with $V_0 = -23$ MeV. The resonance energy and the total width are $E_r = 0.97$ MeV and $\Gamma_{\text{tot}} = 0.98$ MeV, respectively, for $V_0 = -24.5$ MeV, while they are $E_r = 2.07$ MeV and $\Gamma_{\text{tot}} = 0.96$ MeV for $V_0 = -23$ MeV.

$\sqrt{5/3}$ times larger than the radius parameter of the square-well potential). See Ref. [36] for a recent β - γ spectroscopy measurement for the ^{31}Mg nucleus. In the figure, the dashed and the dot-dashed curves show the partial width for the s and d wave channels, respectively, as a function of the resonance energy, E_r . The solid line shows the total width. To evaluate these, we vary the depth parameter of the square-well potential from $V_0 = -24$ MeV to -19 MeV. For each value of V_0 , we first look for the resonance energy, E_r , which satisfies $\det(\mathbf{L}_>(E_r) - S(E_r)) = 0$. We find that this procedure is essential in order to obtain physical values of the partial widths, in contrast to the spherical case in which one can choose V_0 somewhat arbitrarily. After the resonance energy is found in this way, the partial widths are then evaluated according to Eqs. (50), (D9), and (D10). For $E < \epsilon_2$, the d -wave channel

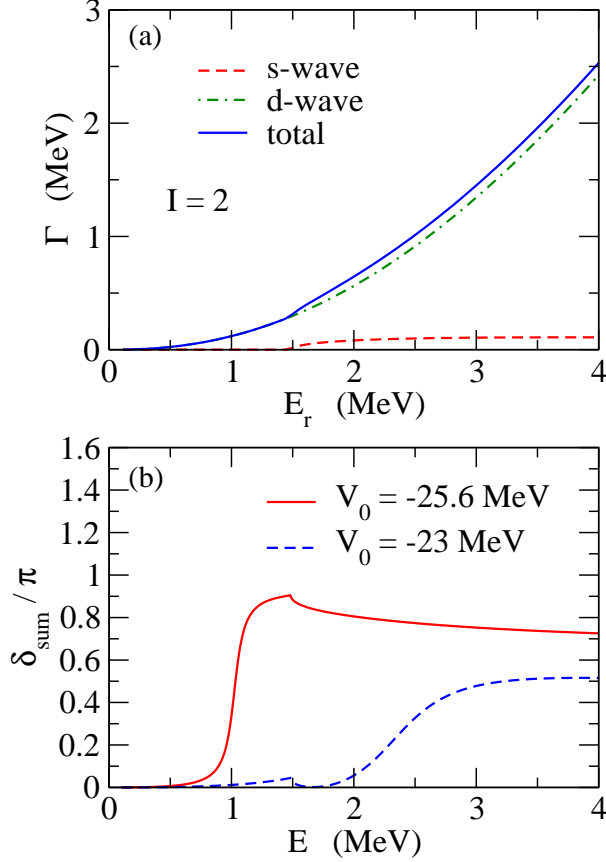


Fig. 4 Same as Fig. 3, but for the total angular momentum of $I = 2$, with channels $|0^+ \otimes d\rangle$ and $|2^+ \otimes s\rangle$. In the lower panel, the eigenphase sums are plotted for $V_0 = -25.6$ MeV and -23 MeV. The resonance energy and the width are $E_r = 0.99$ MeV and $\Gamma_{\text{tot}} = 0.17$ MeV, respectively, for the former potential, while they are $E_r = 2.46$ MeV and $\Gamma_{\text{tot}} = 0.98$ MeV for the latter potential. The kinks at the threshold energy for the excited channel ($E = 1.48$ MeV) are the Wigner cusps.

is closed, and the partial width for this channel is zero. In this case, $S_{l=2}$ is evaluated by changing k_2 in the following formula [4]

$$S_{l=2} = -\frac{18 + 3k_2^2 R^2}{9 + 3k_2^2 R^2 + k_2^4 R^4}, \quad (52)$$

to $i\kappa_2$ with $\kappa_2 = \sqrt{2\mu|E - \epsilon_2|/\hbar^2}$ as

$$S_{l=2} = -\frac{18 - 3\kappa_2^2 R^2}{9 - 3\kappa_2^2 R^2 + \kappa_2^4 R^4}. \quad (53)$$

One can see that the partial width for the d -wave channel becomes dominant as the resonance energy increases, and thus the resonance state gradually changes to a d -wave character as a function of energy. It is interesting to see that the resonance state exists even when the d -wave channel is closed at $E_r < \epsilon_2$. In order to see this more clearly, the lower panel of Fig. 3 shows the eigenphase sum, δ_{sum} , defined as a sum of eigen phase shifts δ_α , that is, $\delta_{\text{sum}} = \sum_\alpha \delta_\alpha$ [17, 29, 30] as a function of energy, E . Here, the eigen phase shifts are

defined as $\lambda_\alpha = e^{2i\delta_\alpha}$, where λ_α is an eigenvalue of the S -matrix. The eigenphase sum is a generalization of the phase shift for a single-channel case, and shows a resonance behavior with the resonance energy E_r and the width Γ_{tot} [29, 30]. In the figure, the solid and the dashed lines are obtained with $V_0 = -24.5$ MeV and -23 MeV, respectively. Here, we calculate the eigenphase sum according to the formula $e^{2i\delta_{\text{sum}}} = \det(\mathbf{U})$ with the S -matrix computed by Eq. (41). For the former value of the potential depth, the resonance energy and the total width are found to be $E_r = 0.97$ MeV and $\Gamma_{\text{tot}} = 0.98$ MeV, respectively, while for the latter they are $E_r = 2.07$ MeV and $\Gamma_{\text{tot}} = 0.96$ MeV. One can see that the eigenphase sum increases rapidly around $E \sim E_r$ for each case, which is expected as a resonance behavior. An interesting thing to see is that the s -wave channel shows a resonance behavior as a consequence of the coupling to the d -wave channel, even when the d -wave channel is kinetically forbidden (that is, a closed channel). Another interesting thing is that the square well potential with $V_0 = -24.5$ MeV does not hold a d -wave bound state. When the energy $E - \epsilon_\alpha$ for a closed channel ($E - \epsilon_\alpha < 0$) coincides with the energy of a bound state, the phase shift for open channels shows a resonance behavior. This is referred to as the Feshbach resonance, and plays an important role in the physics of cold atoms [37]. Since there is no bound state in the present case, the resonance behavior shown by the solid line in the lower panel of Fig. 3 should have a different character from a Feshbach resonance. Notice that the resonance width is a decreasing function of E_r before the d -wave channel is open, i.e., for $E_r < 1.48$ MeV. This is partly due to a strong energy dependence of S_2 given by Eq. (53), which is much stronger than the energy dependence of S_2 for open channels given by Eq. (52).

The resonance widths for the total angular momentum $I = 2$ are shown in the upper panel of Fig. 4. In this case, the channels $|0^+ \otimes d\rangle$ and $|2^+ \otimes s\rangle$ are coupled together. One can see that the resonance width is similar to the single-channel case shown in the lower panel of Fig. 1. That is, the d -wave channel dominates the total width with only a small contribution from the s -wave channel. The eigenphase sums for $V_0 = -25.6$ MeV and $V_0 = -23$ MeV are shown in the lower panel of Fig. 4. The resonance energy and the total width are $E_r = 0.99$ MeV and $\Gamma_{\text{tot}} = 0.17$ MeV, respectively, for the former potential, while they are $E_r = 2.46$ MeV and $\Gamma_{\text{tot}} = 0.98$ MeV for the latter potential. One can clearly see the expected resonance behavior, especially for the former potential with a smaller resonance width. In addition, one can also see a kink at the threshold energy for the excited channel, that is, at $E = \epsilon_2 = 1.48$ MeV. This is nothing but the Wigner cusp, discussed by Wigner in 1948 [38] (see also Ref. [39]).

One may have expected that the resonance width for small resonance energies is determined by the s -wave due to the absence of the centrifugal barrier while the partial width for the d -wave channel is largely suppressed. This was not seen in Fig. 4 due to the threshold energy, because of which the s -wave channel contributes only at energies above the threshold. In order to gain a deeper insight into the role of the s -wave channel, we repeat the same calculation as in Fig. 4, but by setting the excitation energy of the 2^+ state of the core nucleus to be zero. The results are shown in Fig. 5. As expected, the partial width for the s -wave channel is larger than that for the d -wave channel, at energies below about 0.8 MeV. At very low energies, the partial width for the d -wave channel is largely suppressed due to the finite centrifugal barrier. A similar mechanism appears in the two-neutron decay of

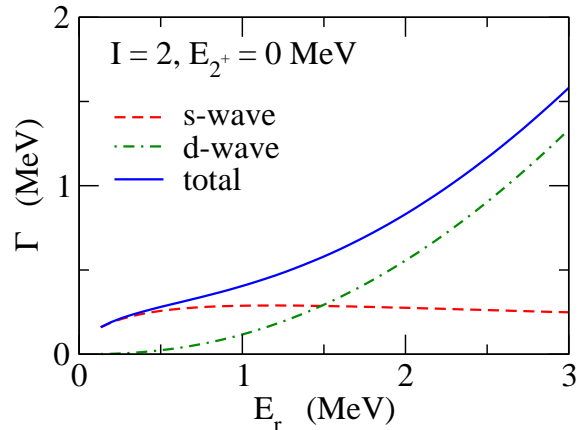


Fig. 5 Same as the upper panel of Fig. 4, but obtained by setting the excitation energy of the core nucleus to be zero.

^{26}O , for which the resonance energy is extremely small and the decay dynamics is largely determined by the s -wave component in the wave function [40, 41].

4. Summary

We have derived a compact formula, Eq. (48), for partial decay widths for a multi-channel resonance state using a deformed square-well potential. This was an extension of the formula derived in Ref. [4] for a single-channel case to a resonance in a particle-core coupling model. We have applied the formula to a two-channel problem with s and d wave couplings. We have shown that, even though a pure s -wave state hardly forms a resonance due to the absence of the centrifugal barrier, a resonance may appear as a consequence of the coupling to the d -wave channel. This is the case even when the d -wave channel is closed and/or there is no bound state in the excited channel. We have also shown that the s -wave component provides a dominant contribution at low energies, whenever it is available, while the resonance changes to a d -wave character as the resonance energy increases.

The resonance formula obtained in this paper is simple and semi-analytic. In particular, one does not need to solve the coupled-channels equations numerically. The formula is thus useful, at least qualitatively, in analyzing experimental data e.g., for beta-delayed neutron emissions from neutron-rich nuclei, even though several approximations used in this paper may have to be carefully examined for quantitative discussions. We will present such analysis in a separate paper.

Acknowledgments

We thank M. Ichimura, I. Hamamoto, and T. Shimoda for useful discussions. This work was supported in part by JSPS KAKENHI Grant Numbers JP16K05367, JP17J02034, and JP18KK0084.

A. Comparison between a square-well and a Woods-Saxon potentials

In this Appendix, we compare the resonance width obtained with the spherical square-well (SW) potential with that with a smooth Woods-Saxon (WS) potential. To this end, we seek

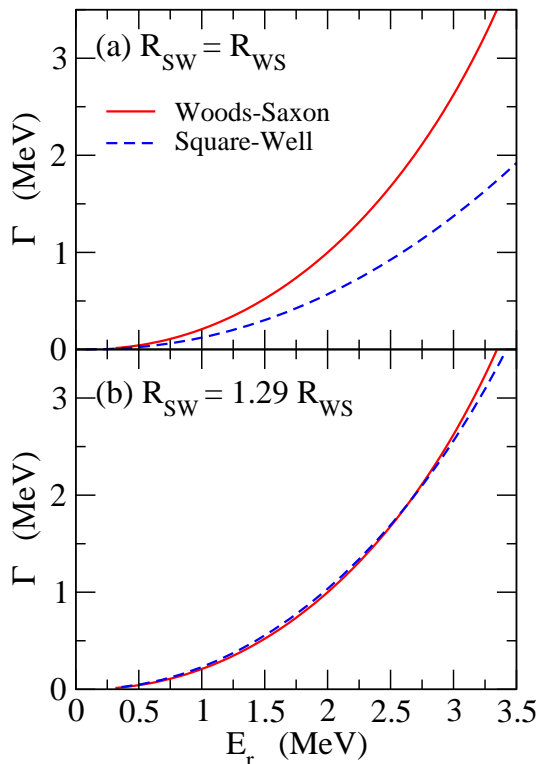


Fig. A1 The resonance widths as a function of the resonance energy for d -wave scattering in the mass region of $A \sim 30$. The solid and the dashed lines show the results of a Woods-Saxon and a square-well potentials, respectively. In the upper panel, the radius of the square-well potential is set to be the same as that of the Woods-Saxon potential, while it is increased by a factor of $\sqrt{5/3}$ in the lower panel.

the d -wave Gamow state for both the potentials (see the dashed line in Fig. 1). For the Woods-Saxon potential, we take the radius and the diffuseness parameter in the Woods-Saxon as $R_{\text{WS}} = 3.95$ fm and $a_{\text{WS}} = 0.67$ fm [4], respectively, and vary the depth parameter, $V_0^{(\text{WS})}$, from -29 MeV to -14 MeV. For the square-well potential, we consider two different choices of the radius parameter, R . One is to take the same value as in the Woods-Saxon potential (the upper panel), and the other is to increase the radius by a factor of $\sqrt{5/3}$ (the lower panel) so that the quantity

$$\langle r^2 \rangle = \frac{\int d\mathbf{r} r^2 V(r)}{\int d\mathbf{r} V(r)} \quad (\text{A1})$$

is approximately the same between the Woods-Saxon and the square-well potentials. For $R = R_{\text{WS}}$, we vary the depth parameter V_0 from -27 MeV to -21 MeV, while we vary it from -16 MeV to -10.5 MeV for $R = \sqrt{5/3}R_{\text{WS}}$.

The solid and the dashed lines in Fig. A1 show the results of the Woods-Saxon and the square-well potentials, respectively. One can see that the resonance width obtained with the square-well potential behaves qualitatively the same as that obtained with the Woods-Saxon potential. For the increased radius parameter (the lower panel), the square well potential reproduces even quantitatively the result of the Woods-Saxon potential, especially for small

values of the resonance width. A similar behavior can be found also in absorption cross sections, which are relevant to astrophysical fusion reactions [42].

B. Matrix elements of the coupling potential

In this Appendix, we give explicit forms of the matrix elements of the coupling potential, Eq. (30), with the channel wave functions given by Eq. (26) [31]. Using Eq. (7.1.6) in Ref. [32], one obtains

$$\begin{aligned} & V_0 R \langle (ljI_c)IM | \sum_m \alpha_{2m} Y_{2m}^* | (l'j'I_c)IM \rangle \\ &= V_0 R (-)^{j'+I_c+I} \begin{Bmatrix} I & I_c & j \\ 2 & j' & I_c \end{Bmatrix} \langle \mathcal{Y}_{jl} || Y_2 || \mathcal{Y}_{j'l'} \rangle \langle \phi_{I_c} || \alpha_2 || \phi_{I_c} \rangle, \end{aligned} \quad (\text{B1})$$

where $\begin{Bmatrix} I & I_c & j \\ 2 & j' & I_c \end{Bmatrix}$ denotes the Wigner's 6- j symbol. The reduced matrix element $\langle \mathcal{Y}_{jl} || Y_2 || \mathcal{Y}_{j'l'} \rangle$ is calculated as [32],

$$\langle \mathcal{Y}_{jl} || Y_2 || \mathcal{Y}_{j'l'} \rangle = \delta_{l+l'+2, \text{even}} (-1)^{\frac{1}{2}+j} \frac{\sqrt{5} \hat{j} \hat{j}'}{\sqrt{4\pi}} \begin{pmatrix} j & 2 & j' \\ 1/2 & 0 & -1/2 \end{pmatrix}, \quad (\text{B2})$$

where the bracket denotes the 3- j symbol, and \hat{j} and \hat{j}' are defined as $\sqrt{2j+1}$ and $\sqrt{2j'+1}$, respectively. In order to evaluate the reduced matrix element, $\langle \phi_{I_c} || \alpha_2 || \phi_{I_c} \rangle$, one needs a specific model for ϕ_{I_c} , which is given below. Notice that the $E2$ transition strength is given by

$$B(E2 : I_c \rightarrow I_c') = \frac{1}{2I_c + 1} |\langle \phi_{I_c} || \hat{T}^{(E2)} || \phi_{I_c'} \rangle|^2, \quad (\text{B3})$$

with the $E2$ operator give by [33]

$$\hat{T}_m^{(E2)} = \frac{3e}{4\pi} Z_c R^2 \alpha_{2m}, \quad (\text{B4})$$

where Z_c is the proton number of the core nucleus.

B.1. Vibrational coupling

We first discuss the vibrational coupling of spherical nuclei. In this case, the surface coordinate α_{2m} is regarded as a coordinate for a harmonic oscillator. It is related to the phonon creation and annihilation operators as [33]

$$\alpha_{2m} = \frac{\beta_2}{\sqrt{5}} \left(a_{2m}^\dagger + (-1)^m a_{2-m} \right), \quad (\text{B5})$$

where $\beta_2/\sqrt{5}$ is the amplitude of the zero-point motion. The ground state with $I_c = 0$ and the one phonon state with $I_c = 2$ are given as,

$$|\phi_{00}\rangle = |0\rangle, \quad (\text{B6})$$

$$|\phi_{2m}\rangle = a_{2m}^\dagger |0\rangle, \quad (\text{B7})$$

respectively, where $|0\rangle$ is the vacuum state for the harmonic oscillator. From these wave functions, one finds

$$\langle \phi_2 || \alpha_2 || \phi_0 \rangle = \beta_2, \quad (\text{B8})$$

and thus [11]

$$V_0 R \langle (I j I_c = 2) IM | \sum_m \alpha_{2m} Y_{2m}^* | (I' j' I'_c = 0) IM \rangle = V_0 R \frac{\beta_2}{\sqrt{4\pi}} \left\langle j' \frac{1}{2} 20 \left| j \frac{1}{2} \right. \right\rangle. \quad (\text{B9})$$

In the vibrational model, there is no coupling from the one phonon state to the same state (that is, the reorientation term). From Eq. (B3), the value of β_2 can be estimated from a measured $B(E2)$ strength from the ground state to the one phonon state, $B(E2) \uparrow$, as [31]

$$\beta_2 = \frac{4\pi}{3Z_c R^2} \sqrt{\frac{B(E2) \uparrow}{e^2}}. \quad (\text{B10})$$

In a similar way, the wave function for the two phonon states is given as,

$$|\phi_{2\text{ph}:I_c M_c}\rangle = \frac{1}{\sqrt{2}} [a_2^\dagger a_2^\dagger]^{(I_c M_c)} |0\rangle, \quad (\text{B11})$$

from which one finds

$$\langle \phi_{2\text{ph}:I_c} | \alpha_2 | \phi_{1\text{ph}:I_c=2} \rangle = \sqrt{\frac{2(2I_c + 1)}{5}} \beta_2. \quad (\text{B12})$$

Similar to the 1 phonon state, there is no coupling among the 2 phonon states, as well as the coupling between the 2 phonon states and the ground state.

B.2. Rotational coupling

We next consider the rotational coupling of deformed nuclei. In this case, we first transform the surface coordinate α_{2m} to the body-fixed coordinate as

$$a_{2m} = \sum_{m'} D_{m'm}^2(\varphi_d, \theta_d, \chi_d) \alpha_{2m'}, \quad (\text{B13})$$

where φ_d, θ_d , and χ_d are the Euler angles which specify the body-fixed frame, and $D_{m'm}^2$ is the Wigner's D -function. For axial deformation, only the $m = 0$ component in a_{2m} is finite. In this case, one has

$$\alpha_{2m} = \beta_2 \sqrt{\frac{4\pi}{5}} Y_{2m}(\theta_d, \varphi_d), \quad (\text{B14})$$

with $a_{20} = \beta_2$ being a deformation parameter. For the ground state rotational band in even-even nuclei, the wave function of the rotational states reads

$$|\phi_{I_c M_c}\rangle = |Y_{I_c M_c}\rangle, \quad (\text{B15})$$

and one obtains

$$\langle \phi_{I_c} | \alpha_2 | \phi_{I'_c} \rangle = \beta_2 \sqrt{\frac{4\pi}{5}} \langle Y_{I_c} | Y_2 | Y_{I'_c} \rangle = (-)^{I_c} \beta_2 \hat{I}_c \hat{I}'_c \begin{pmatrix} I_c & 2 & I'_c \\ 0 & 0 & 0 \end{pmatrix}, \quad (\text{B16})$$

with

$$\langle Y_l | Y_2 | Y_{l'} \rangle = (-1)^l \frac{\sqrt{5} \hat{l}'}{\sqrt{4\pi}} \begin{pmatrix} l & 2 & l' \\ 0 & 0 & 0 \end{pmatrix}. \quad (\text{B17})$$

Notice that the relation between the deformation parameter β_2 and the $B(E2)$ value is the same as in the vibrational case, Eq. (B10). The coupling matrix element between the ground state and the first 2^+ state is also the same as in the vibrational case and is given by Eq. (B9). A difference from the vibrational coupling comes from the reorientation term, that is, the self-coupling from the 2^+ state to the same state [31].

C. Matrix elements with the channel wave functions of Eq. (27)

In this Appendix, we give the matrix elements with the channel wave functions given by Eq. (27) instead of Eq. (26). The equation which corresponds to Eq. (B1) in Appendix B then reads

$$\begin{aligned} & V_0 R \langle (lI_c)IM | \sum_m \alpha_{2m} Y_{2m}^* | (l'I_c)IM \rangle \\ &= V_0 R (-)^{l'+I_c+I} \begin{Bmatrix} I & I_c & l \\ 2 & l' & I_c \end{Bmatrix} \langle Y_l || Y_2 || Y_{l'} \rangle \langle \phi_{I_c} || \alpha_2 || \phi_{I_c} \rangle. \end{aligned} \quad (C1)$$

The equation that corresponds to Eq. (B9) in Appendix B reads

$$V_0 R \langle (lI_c = 2)IM | \sum_m \alpha_{2m} Y_{2m}^* | (l'I_c = 0)IM \rangle = V_0 R \frac{\beta_2}{\sqrt{4\pi}} \langle l'020 | l0 \rangle, \quad (C2)$$

both for the vibrational and for the rotational couplings. For the rotational coupling, the reorientation term with $l = l' = 2$, $I_c = I'_c = 2$ and $I = 0$ is given by [31]

$$V_0 R \langle [d \otimes 2^+]^{(00)} | \sum_m \alpha_{2m} Y_{2m}^* | [d \otimes 2^+]^{(00)} \rangle = V_0 R \frac{2}{7} \sqrt{\frac{5}{4\pi}} \beta_2. \quad (C3)$$

The reorientation term with $l = l' = 0$ vanishes due to the selection rule of angular momentum.

D. Two-channel coupling

When only two-channels are involved in the coupling, the matrix $\mathbf{L}_> - \mathbf{S}$ in Eq. (47) is a 2×2 matrix, whose inverse can be explicitly written down. The matrix $\mathbf{L}_> - \mathbf{S}$ has components given by

$$(\mathbf{L}_> - \mathbf{S})_{11} = \frac{2\mu}{\hbar^2} RC_{11} + L_1 - S_1, \quad (D1)$$

$$(\mathbf{L}_> - \mathbf{S})_{22} = \frac{2\mu}{\hbar^2} RC_{22} + L_2 - S_2, \quad (D2)$$

$$(\mathbf{L}_> - \mathbf{S})_{12} = (\mathbf{L}_> - \mathbf{S})_{21} = \frac{2\mu}{\hbar^2} RC_{12}, \quad (D3)$$

where S_i ($i = 1, 2$) are given by Eq. (8) while L_i ($i = 1, 2$) are given by

$$L_i = 1 + K_i R \frac{j'_i(K_i R)}{j_i(K_i R)}. \quad (D4)$$

The determinant of the matrix $\mathbf{L}_> - \mathbf{S}$ reads

$$\det(\mathbf{L}_> - \mathbf{S}) = (\mathbf{L}_> - \mathbf{S})_{11}(\mathbf{L}_> - \mathbf{S})_{22} - (\mathbf{L}_> - \mathbf{S})_{12}^2. \quad (D5)$$

Notice that the energy derivative of L_i is given as

$$\frac{\partial L_i}{\partial E} = -\frac{\mu R}{\hbar^2} \left[1 - \frac{l_i(l_i + 1)}{K_i^2 R^2} + \frac{1}{K_i R} \frac{j'_i(K_i R)}{j_i(K_i R)} + \left(\frac{j'_i(K_i R)}{j_i(K_i R)} \right)^2 \right]. \quad (D6)$$

In the spherical case, one can use the resonance condition, $L_i = S_i$, to obtain the approximate formula for $\frac{\partial L_i}{\partial E}$ [4]. In contrast, in the multi-channel case, the resonance condition is

somewhat more complicated, that is, $\det(\mathbf{L}_> - \mathbf{S}) = 0$, and a simple approximate formula for $\frac{\partial L_i}{\partial E}$ cannot be obtained.

Since the elements of the cofactor matrix of the 2×2 matrix $\mathbf{L}_> - \mathbf{S}$ are given by

$$\text{cof}(\mathbf{L}_> - \mathbf{S})_{11} = (\mathbf{L}_> - \mathbf{S})_{22}, \quad (\text{D7})$$

$$\text{cof}(\mathbf{L}_> - \mathbf{S})_{22} = (\mathbf{L}_> - \mathbf{S})_{11}, \quad (\text{D8})$$

the γ_i^2 in Eq. (48) reads

$$\gamma_1^2 = -\frac{\frac{2\mu}{\hbar^2}RC_{22} + L_2 - S_2}{\frac{d}{dE}\det(\mathbf{L}_> - \mathbf{S})|_{E=E_r}}, \quad (\text{D9})$$

$$\gamma_2^2 = -\frac{\frac{2\mu}{\hbar^2}RC_{11} + L_1 - S_1}{\frac{d}{dE}\det(\mathbf{L}_> - \mathbf{S})|_{E=E_r}}, \quad (\text{D10})$$

where the numerators are evaluated at $E = E_r$. The partial and the total widths are then evaluated according to Eqs. (50) and (51), respectively.

In the no-coupling limit, the coupling matrix \mathbf{C} vanishes, and thus the determinant of $\mathbf{L}_> - \mathbf{S}$ becomes

$$\det(\mathbf{L}_> - \mathbf{S}) = (L_1 - S_1)(L_2 - S_2). \quad (\text{D11})$$

Suppose that $L_1 - S_1 = 0$ at $E = E_r$. Then, the energy derivative of the determinant reads

$$\frac{d}{dE}\det(\mathbf{L}_> - \mathbf{S})|_{E=E_r} = -\frac{1}{\gamma_{l_1}^2}(L_2 - S_2), \quad (\text{D12})$$

where $\gamma_{l_1}^2$ is given by Eq. (15). This leads to $\gamma_1^2 = \gamma_{l_1}^2$ and $\gamma_2^2 = 0$, which is consistent with the single-channel case discussed in Sec. II.

References

- [1] M. Pfützner, M. Karny, L.V. Grigorenko, and K. Riisager, *Rev. Mod. Phys.* **84**, 567 (2012).
- [2] P.J. Woods and C.N. Davids, *Ann. Rev. Nucl. Part. Sci.* **47**, 541 (1997).
- [3] T. Nakamura, H. Sakurai, and H. Watanabe, *Prog. in Part. and Nucl. Phys.* **97**, 53 (2017).
- [4] A. Bohr and B.R. Mottelson, *Nuclear Structure* (W.A. Benjamin, Reading, MA, 1969), Vol. I, Appendix 3F-2 and p. 239.
- [5] D.J. Millener, C.B. Dover, and A. Gal, *Prog. Theo. Phys. Suppl.* **117**, 307 (1994).
- [6] A.T. Kruppa, B. Barmore, W. Nazarewicz, and T. Vertse, *Phys. Rev. Lett.* **84**, 4549 (2000).
- [7] B. Barmore, A.T. Kruppa, W. Nazarewicz, and T. Vertse, *Phys. Rev.* **C62**, 054315 (2000).
- [8] E. Maglione and L.S. Ferreira, *Phys. Rev.* **C61**, 047307 (2000).
- [9] C.N. Davids and H. Esbensen, *Phys. Rev.* **C61**, 054302 (2000).
- [10] H. Esbensen and C.N. Davids, *Phys. Rev.* **C63**, 014315 (2000).
- [11] C.N. Davids and H. Esbensen, *Phys. Rev.* **C64**, 034317 (2001).
- [12] K. Hagino, *Phys. Rev.* **C64**, 041304 (2001).
- [13] M. Karny *et al.*, *Phys. Rev. Lett.* **90**, 012502 (2003).
- [14] K. Fossez, J. Rotureau, N. Michel, Q. Liu, and W. Nazarewicz, *Phys. Rev.* **C94**, 054302 (2016).
- [15] S.M. Wang and W. Nazarewicz, *Phys. Rev. Lett.* **120**, 212502 (2018).
- [16] E. Maglione, L.S. Ferreira, and R.J. Liotta, *Phys. Rev. Lett.* **81**, 538 (1998); *Phys. Rev.* **C59**, R589 (1999).
- [17] K. Hagino and Nguyen Van Giai, *Nucl. Phys.* **A735**, 55 (2004).
- [18] K. Yoshida and K. Hagino, *Phys. Rev.* **C72**, 064311 (2005).
- [19] I. Hamamoto, *Phys. Rev.* **C72**, 024301 (2005); *Phys. Rev.* **C73**, 064308 (2006); *Phys. Rev.* **C77**, 054311 (2008).
- [20] We follow Ref. [21] to use the phase convention for the spherical Neumann function, with which the asymptotic form is given by $n_l(kr) \rightarrow -\cos(kr - l\pi/2)$ ($r \rightarrow \infty$). Notice that this is a different sign convention from that used in Ref. [4].
- [21] M. Abramowicz and I.A. Stegun, *Handbook of Mathematical Functions* (Dover, New York, 1972).

-
- [22] I.J. Thompson and F.M. Nunes, *Nuclear Reactions for Astrophysics* (Cambridge University Press, New York, 2009).
- [23] A.M. Lane and R.G. Thomas, *Rev. Mod. Phys.* **30**, 257 (1958).
- [24] P. Descouvemont and D. Baye, *Rep. Prog. Phys.* **73**, 036301 (2010).
- [25] A.T. Kruppa and W. Nazarewicz, *Phys. Rev. C***69**, 054311 (2004).
- [26] Y. Takeichi, T. Une, K. Nakamura, T. Kohmura, and T. Miyazima, *Prog. Theo. Phys.* **48**, 858 (1972).
- [27] B.R. Johnson, *J. Chem. Phys.* **69**, 4678 (1978).
- [28] J.R. Taylor, *Scattering Theory: The Quantum Theory on Nonrelativistic Collisions* (Wiley, New York, 1972), Ch. 20.
- [29] H.A. Weidenmüller, *Phys. Lett.* **24B**, 441 (1967).
- [30] A.U. Hazi, *Phys. Rev.* **A19**, 920 (1979).
- [31] K. Hagino and N. Takigawa, *Prog. Theo. Phys.* **128**, 1061 (2012).
- [32] A.R. Edmonds, *Angular Momenta in Quantum Mechanics*, (Princeton University Press, Princeton N.J., 1957).
- [33] P. Ring and P. Schuck, *The Nuclear Many Body Problem* (Springer-Verlag, New York, 1980).
- [34] O. Nidermaier *et al.*, *Phys. Rev. Lett.* **94**, 172501 (2005).
- [35] H. Mach *et al.*, *Eur. Phys. J.* **A25**, 105 (2005).
- [36] H. Nishibata, S. Kanaya, T. Shimoda, A. Odahara, S. Morimoto, A. Yagi, H. Kanaoka, M.R. Pearson, C.D.P. Levy, M. Kimura, N. Tsunoda, and T. Otsuka, *Phys. Rev. C***99**, 024322 (2019).
- [37] C. Chin, R. Grimm, P. Julienne, and E. Tiesinga, *Rev. Mod. Phys.* **82**, 1225 (2010).
- [38] E.P. Wigner, *Phys. Rev.* **73**, 1002 (1948).
- [39] N. Michel, W. Nazarewicz, and M. Płoszajczak, *Phys. Rev. C***75**, 031301(R) (2007).
- [40] K. Hagino and H. Sagawa, *Phys. Rev. C***89**, 014331 (2014); **C93**, 034330 (2016).
- [41] L.V. Grigorenko, I.G. Mukha, and M.V. Zhukov, *Phys. Rev. Lett.* **111**, 042501 (2013).
- [42] R. Ogura, K. Hagino, and C.A. Bertulani, *Phys. Rev. C***99**, 065808 (2019).